

# Preparation and Characterization of Supercritical CO<sub>2</sub> Nanocellulose Aerogels

Jing Luo<sup>a,b</sup>, Hua Wang<sup>a,\*</sup>

<sup>a</sup>Metallurgical and Energy Engineering College, Kunming University of Science and Technology, Kunming 650093, China

<sup>b</sup>Fire Protection Institute, Southwest Forestry University, Kunming 650024, China

[lincoln558@163.com](mailto:lincoln558@163.com)

This paper uses poplar wood chips as raw materials to prepare nanocellulose (NCC) by sulfuric acid hydrolysis, and then through physical gelling of inorganic salt solution, tert-butyl alcohol (TBA) replacement and supercritical CO<sub>2</sub> drying to prepare the nanocellulose aerogels. The characterization analysis and performance test of nanocellulose aerogels were carried out by field emission scanning electron microscope (FESEM), universal mechanical test machine, automatic specific surface area analyzer and thermogravimetric analyzer. The results show that the prepared nanocellulose aerogels are spherical white particles, and the internal structure of the aerogels is a three-dimensional network structure with no collapse, the specific surface area of the aerogels is between 263.5~358.73 cm<sup>2</sup>/g, and the diameter of the pores mainly distributes between 15~41 nm; as the mass fraction of nanocellulose increases, the compressive strength of the aerogels increases as well and reaches a maximum at 2.39 MPa, the nanocellulose aerogels with a mass fraction of 2.5% have a maximum adsorption capacity of 374 cm<sup>3</sup>/g.

## 1. Introduction

As a new type of third-generation aerogel material, cellulose aerogel not only has the excellent performance of the traditional aerogels, but also integrates some excellent properties of cellulose, such as sufficient raw material, biodegradability, renewable and good biocompatibility, so that it has a wide application prospect (Jin et al., 2004).

The early cellulose aerogels were prepared by the sol-gel method (Lee et al., 2015), namely to dissolve cellulose derivatives into the organic solvent, the wet gels were formed by chemical crosslink reaction and then dried to obtain the aerogels. The selection of chemical crosslink agent and the control of its concentration have important effects on the strength, specific surface area and porosity of the cellulose aerogels (Lopes et al., 2014). However, the disadvantage of sol-gel method is that the preparation process is rather complex, and the pore structure of aerogels is difficult to be precisely controlled (Wan et al., 2015).

The preparation of cellulose aerogels is mainly through two ways, cellulose aqueous partitioning and direct dissolution (Hoepfner et al., 2008; Belhadj et al., 2017). Pääkkö et al. (2010) took cellulose nanofibers as the basic unit to prepare the cellulose aerogels by two drying methods: deep freeze drying and vacuum freeze drying. The aerogels have good flexibility and can be bent many times without broken. Moreover, wet cellulose gels can also be formed at low concentration, and the drying shrinkage rate is also small. Jin et al. (2004) investigated the effects of three drying methods on the porosity and nitrogen adsorption properties of cellulose aerogels. Compared with conventional freeze-drying, solvent replacement drying can effectively maintain the original network morphology inside the wet gels, so that the gels have high porosity and their specific surface area is much higher than that of the conventional freeze-drying aerogel; while rapid freeze drying can only partially maintain the initial network structure of the wet gels, and the microscopic pore structure of aerogels shows uneven characteristics.

Based on this, this paper uses poplar wood chips as raw materials to prepare nanocellulose by sulfuric acid hydrolysis, and then prepare nanocellulose aerogels by supercritical CO<sub>2</sub> drying. Under the premise of full utilization of waste resources, a new green environmental-protection technology is provided for the preparation of nanocellulose aerogels.

## 2. Experiment

### 2.1 Experimental method

#### 2.1.1 Inorganic salt-induced formation mechanism

When forming in the inorganic salt solution, the electrolyte changes the charge distribution of the original sol system so that cellulose molecules get close to each other easily to form gels. The basic reason of inorganic salt's ability to induce and promote the gelation of cellulose solution is that the inorganic salt changes the charge distribution of the original sol system and destroys the stability of the sol system (Wei and Wang, 2013).

#### 2.1.2 Preparation of nanocellulose and formation of hydrogels

Put 5 g of poplar wood chips and 1.5 mol/L ammonium persulfate solution into a 500 mL three-necked flask at a solid-liquid ratio (g:mL) of 1:100, stir the mixture in a 70°C water bath for 30 min, and then prepare the nanocellulose by centrifugation and drying. Weigh 10g nanocellulose, prepare nanocellulose suspensions with mass fractions of 1.5%, 2.5%, and 3.5%, respectively, soak in an ice bath for 15 min ultrasonic processing, after resting for 30 min, add a certain amount of nanocellulose suspensions into 0.25 mol/L CaCl<sub>2</sub> solution, let stand for 48h to fully gel. Spherical hydrogels are prepared using inorganic salt-induced formation principles.

#### 2.1.3 Gel replacement

Perform gel replacement in TBA by multi-step displacement method. Soak the prepared hydrogels in the TBA solution (mass fraction 25%, temperature 40°C), change the mass fraction of TBA every 48h (respectively are 50%, 75% and 100%), remain the other conditions unchanged, at last, obtain the spherical nanocellulose alcohol gels.

#### 2.1.4 Supercritical CO<sub>2</sub> drying

Use supercritical extractor (SFT-105, USA) to perform supercritical CO<sub>2</sub> drying on the prepared nanocellulose alcohol gels. After heating the reactor to 40°C, put the nanocellulose alcohol gels into the reactor (atmosphere of CO<sub>2</sub>, pressure of 12 MPa) and dry for 3h, then obtain the nanocellulose aerogels.

### 2.2 Performance test and characterization

Use blade to cut aerogels with different concentrations, then use double-side tap to fix them on the sample holder and treat with metal spray. Observe the internal microstructure of nanocellulose aerogels with different mass fraction by FESEM (LEO 1530Vp).

Use universal mechanical test machine (CMT-4204, Shanghai) to test the mechanical properties of nanocellulose aerogels with different mass fraction, compress the samples at a rate of 1 mm/min and stop when the diameter is 70% of the initial value.

The specific surface area, pore volume, and pore size distribution of the aerogels with different mass fractions were determined using an automatic specific surface analyzer (ASAP 2020, USA). The degassing temperature was 90° C, degassing time was 48 h. The adsorbed gas was N<sub>2</sub> and the temperature was maintained at 77K.

The TG-DTA curve of the sample is measured by thermogravimetric analyzer (TG-209F3). The flow rate of nitrogen flow was 30 cm<sup>3</sup>/ min, and the heating rate was 15 K / min.

## 3. Results and analysis

Figure 1 (a) is a macroscopic diagram of nanocellulose aerogels prepared by supercritical drying. According to the macroscopic diagram we can see that, the nanocellulose aerogels are white oval particles. The figures (b, c, d) are micrographs of the nanocellulose aerogels with different mass fraction. It can be seen from the figures that the interior of the aerogel is a three-dimensional network structure without collapse. In the process of inorganic salt gelling, the cellulose is interwoven with each other by the hydrogen bonds formed by hydroxyl groups, forming a three-dimensional network structure (Nguyen et al., 2014) with cellulose as the basic skeleton. It can be seen from the diagrams that when the mass fraction of cellulose is 1.5%, it is obvious that the inner pore structure of the aerogels is very sparse, while the internal structure is more dense and the difference is not very large when the mass fraction is 2.5% and 3.5%, and the concentration of cellulose will only affect the density of the network structure of the aerogels and the size of the pore, not its morphology.

Figure 2 is the compression-deformation curve of nanocellulose aerogels with different mass fraction. Because the internal structure of the aerogel is a three-dimensional network structure composed of nanocellulose, the porosity is relatively larger, so the compressive strength is relatively smaller. As can be seen from Figure 2, the compressive strength of the nanocellulose aerogels with mass fraction of 1.5%, 2.5%

and 3.5% is 1.15 MPa, 2.12 MPa and 2.39 MPa, respectively, and the compressive strength of the aerogels increases with the increase of nanocellulose mass fraction. When the mass fraction of nanocellulose increases from 1.5% to 2.5%, the increase of the compressive strength of aerogels is greater than that from 2.5% to 3.5%. It is considered that the internal structure of the aerogel is sparser when the mass fraction of nanocellulose is lower, and the internal structure is denser when the concentration increases, but when the mass fraction reaches a certain value, the internal structure is very dense already, so the increasing effect is not very obvious (Shang et al., 2018).

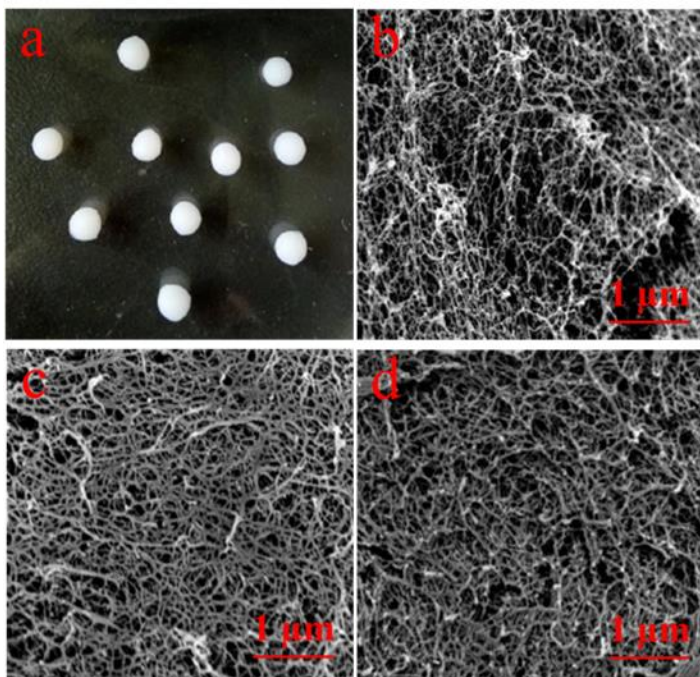


Figure 1: Macroscopic morphology of cellulose aerogels (a) and the micrographs of aerogels with different mass fractions (b, c, d).

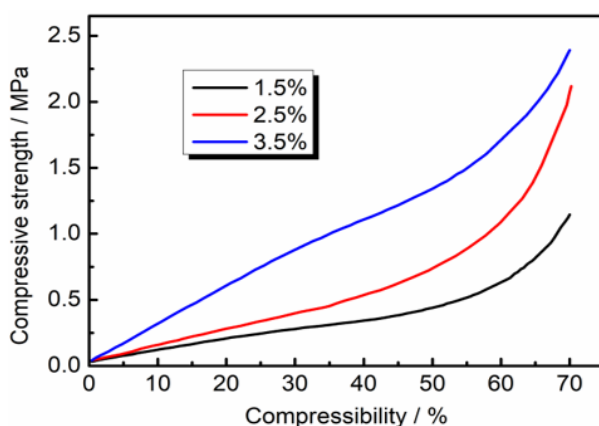


Figure 2: Compression-deformation curves of nanocellulose aerogels with different mass fractions

As can be seen from Figure 3, the adsorption isotherm types of the three different concentrations of spherical nanocellulose aerogels are the same, that is, in the low-pressure region of the adsorption isotherms (0.0-0.1), the adsorption increases sharply within a small section for all cases, indicating that there is a small amount of micropores in the aerogels, mainly the adsorption of monomolecular layers (Meena et al., 2005). It can also be seen from the figure that, for the  $N_2$  adsorption isotherms of aerogels with three different concentration, in the mid-high-pressure region, there are adsorption hysteresis loops for all cases, namely the loops generated by

the separation of adsorption branch and desorption branch of adsorption isotherms. By comprehensive analysis of the adsorption hysteresis loop shapes of three different concentrations of spherical nanocellulose aerogels, we can conclude that they are all close to the hysteresis loop type II, indicating that the aerogels have a rich mesoporous structure.

The pore size distribution of nanocellulose aerogels with different mass fraction was calculated by BJH (Yu et al., 2009) method, as shown in Figure 4. It can be seen from the figure that the aerogels with a mass fraction of 1.5% have an obvious distribution peak around 32 nm and the distribution peak is the strongest, indicating there are many mesoporous pores with a diameter of 32 nm inside; aerogels with a mass fraction of 2.5% have a distinct peak of distribution around 13 nm, and the distribution peak is the strongest, indicating that there are many mesoporous pores with a diameter of 13 nm inside; aerogels with a mass fraction of 3.5% have a distinct peak of distribution around 41 nm, and the distribution peak is the strongest, indicating that there are many mesoporous pores with a diameter of 41 nm inside. In addition, in the other pore diameter range (<100 nm), the nanocellulose aerogels with different mass fraction have different pore sizes distribution, indicating that the pores inside the aerogel are relatively uniform, mainly are mesopores.

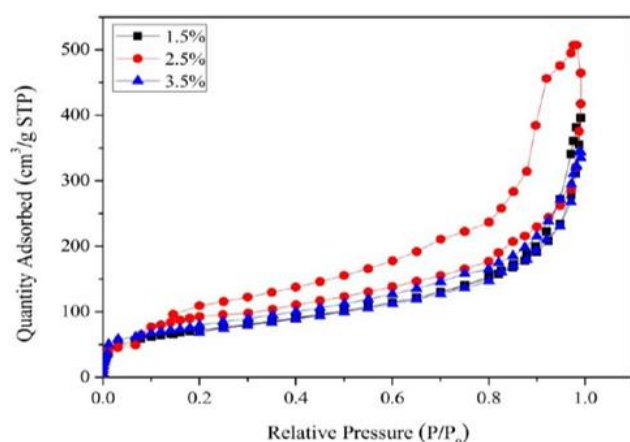


Figure 3:  $N_2$  adsorption-desorption curves of nanocellulose aerogels with different mass fractions

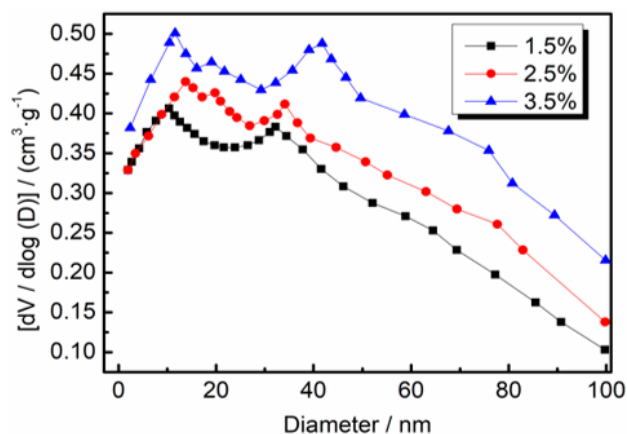


Figure 4: Pore size distribution of nanocellulose aerogels

The thermogravimetric (TGA) and derivative thermogravimetric (DTG) curves of cellulose aerogels are shown in Figure 5, and the thermogravimetric analysis curves of all samples can be divided into 3 stages, (Yang and Cheng, 2009). The first stage: from room temperature to 250°C, the mass loss is about 10%, mainly due to the evaporation of adsorbed water. The second stage: the temperature range of 250~400°C, it is mainly the pyrolysis stage of the cellulose, including the depolymerization, dehydration and decomposition of the glucose molecular chain, and finally the carbonized residue is formed. The third stage: when the temperature is higher

than 400°C, the carbonized residue oxidatively decomposes into low molecular weight gaseous products, the residual part is aromatic-cyclized to form graphite structure gradually. Nanocellulose is obtained by sulfuric acid hydrolysis of microcrystalline cellulose. After sulfuric acid hydrolysis, since the surface of nanocellulose has been partially sulfated, a certain amount of sulfonic acid ester group is introduced, and the degree of polymerization of nanocellulose is reduced and the specific surface area is increased, the ratio of the reduction end on the surface to the exposed reactive active group is increased, resulting in decrease of its thermal stability.

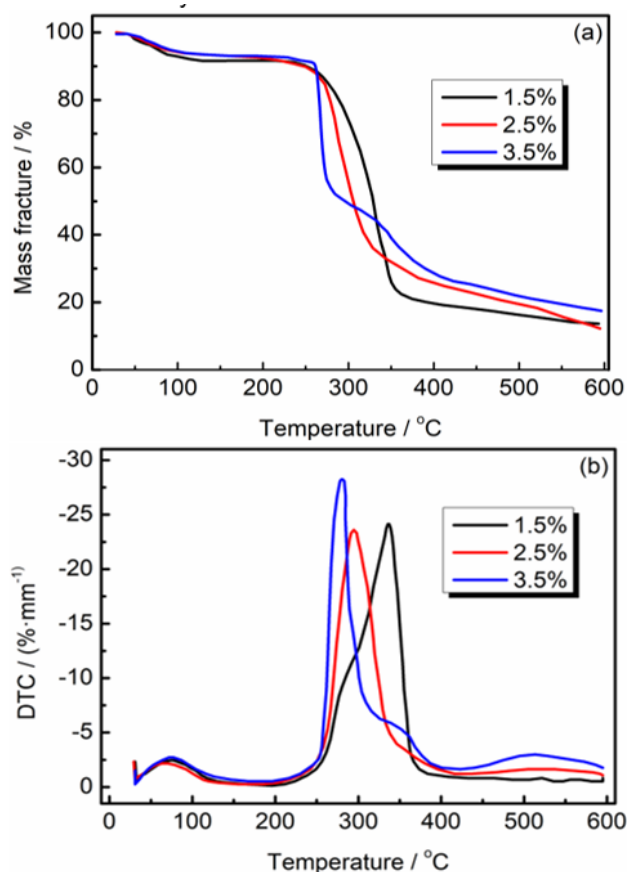


Figure 5: Thermogravimetric curves (a) and derivative thermogravimetric curves (b) of nanocellulose aerogels with different mass fractions

#### 4. Conclusion

This experiment takes the poplar wood chips as raw materials to obtain nanocellulose by sulfuric acid hydrolysis. By physical gelling of inorganic salt solution, TBA replacement and supercritical CO<sub>2</sub> drying, it successfully prepared the spherical cellulose aerogels.

- 1) The analysis showed that, for the aerogels prepared by supercritical CO<sub>2</sub> drying, the inside is sparse, porous, layered three-dimensional structures with a few three-dimensional network structures.
- 2) Spherical nanocellulose aerogels have a high compressive strength, which increases with the increase of the mass fraction of cellulose (1.5%, 2.5%, 3.5%), respectively are 1.15, 2.12 and 2.39MPa.
- 3) The specific surface area and average pore volume of cellulose aerogels increase with the increase of cellulose mass fraction, and the average pore size decreases with the increase of mass fraction. The specific surface area is between 263.25 cm<sup>2</sup>/g and 358.73 cm<sup>2</sup>/g, and the average pore volume is between 0.5176 cm<sup>3</sup>/g and 0.7635 cm<sup>3</sup>/g, and the average pore size is in the range of 15.2 nm to 41.6 nm.
- 4) Thermogravimetric analysis showed that the thermal stability of cellulose aerogels with different mass fraction had no obvious difference, and the maximum mass loss temperature was 275°C.

## Acknowledgements

This work was supported financially by the Yunnan Science and Technology Plan Surface Project of China (No. 2015FB151).

## References

- Belhadj A., Boukhalifa A., Belalia S.A., 2017, Free vibration modelling of Single-walled Carbon Nanotubes using the Differential Quadrature Method, *Mathematical Modelling of Engineering Problems*, 4(1), 33-37, DOI: 10.18280/mmep.040107
- Carotenuto C., Guarino G., Minale M., Morrone B., 2016, Biogas production from anaerobic digestion of manure at different operative conditions, *International Journal of Heat and Technology*, 34(4), 623-629, DOI: 10.18280/ijht.340411
- Hoepfner S., Ratke L., Milow B., 2008, Synthesis and characterisation of nanofibrillar cellulose aerogels, *Cellulose*, 15(1), 121-129, DOI: 10.1007/s10570-007-9146-8
- Jin H., Nishiyama Y., Wada M., Kuga S., 2004, Nanofibrillar cellulose aerogels, *Colloids & Surfaces A Physicochemical & Engineering Aspects*, 240(1), 63-67, DOI: 10.1016/j.colsurfa.2004.03.007
- Jin H., Nishiyama Y., Wada M., Kuga S., 2004, Nanofibrillar cellulose aerogels, *Colloids & Surfaces A Physicochemical & Engineering Aspects*, 240(1), 63-67, DOI: 10.1016/j.colsurfa.2004.03.007
- Lee S., Jeong M.J., Kang K.Y., 2015, Preparation of cellulose aerogels as a nano-biomaterial from lignocellulosic biomass, *Journal of the Korean Physical Society*, 67(4), 738-741, DOI: 10.3938/jkps.67.738
- Lopes J.M., Mustapa A.N., Pantić M., Bermejo, M.D., Martin A., 2017, Preparation of cellulose aerogels from ionic liquid solutions for supercritical impregnation of phytol, *Journal of Supercritical Fluids*, 130, DOI: 10.1016/j.supflu.2017.07.018
- Meena A.K., Mishra G.K., Rai P.K., Rajagopal C., Nagar P.N., 2005, Removal of heavy metal ions from aqueous solutions using carbon aerogel as an adsorbent, *Journal of Hazardous Materials*, 122(1), 161-170, DOI: 10.1016/j.jhazmat.2005.03.024
- Nguyen S.T., Feng J., Shao K.N., Wong J.P.W., Tan, V.B.C., Duong H.M., 2014, Advanced thermal insulation and absorption properties of recycled cellulose aerogels, *Colloids & Surfaces A Physicochemical & Engineering Aspects*, 445(6), 128-134, DOI: 10.1016/j.colsurfa.2014.01.015
- Paakko M., Vapaavuori J., Silvennoinen R., Houbenov N., Ras R.H.A., 2010, Flexible and hierarchically porous nanocellulose aerogels: Templates for functionalities, *Abstracts of papers of the American Chemical Society*, 239.
- Shang J., Yang Q.S., Liu X., Wang C., 2018, Compressive deformation mechanism of honeycomb-like graphene aerogels, *Carbon*, 134, 398-410, DOI: 10.1016/j.carbon.2018.04.013
- Wan C., Lu Y., Cao J., 2015, Preparation, characterization and oil adsorption properties of cellulose aerogels from four kinds of plant materials via a NaOH/PEG aqueous solution, *Fibers & Polymers*, 16(2), 302-307.
- Wang D., Zhang Y.D., Adu E., Yang J.P., Shen Q.W., Tian L., Wu L.J., 2016, Influence of dense phase CO<sub>2</sub> pipeline transportation parameters, *International Journal of Heat and Technology*, 34(3), 479-484, DOI: 10.18280/ijht.340318
- Wei Z.P., Wang T., 2013, Preparation of cellulose aerogel by the salt-induced gelation, *Chinese Journal of Process Engineering*, 13, 351-355.
- Yang J., Chen J., 2009, Fourier transform infrared spectroscopy and thermal analysis of silica aerogel modified by methyl groups, *Journal of Xian Jiaotong University*.
- Yu Z., Carter R.N., Zhang J., 2009, Measurements of Effective Oxygen Diffusivity, Pore Size Distribution, and Porosity in PEM Fuel Cell Electrodes, *Fuel Cells*, 12, 557-565, DOI: 10.1002/uce.201200017